J. Braz. Chem. Soc., Vol. 22, No. 2, S1-S20, 2011.
Printed in Brazil - ©2011 Sociedade Brasileira de Química
0103 - 5053 $6.00+0.00

Supplementary Information

Chlorination of Isatins with Trichloroisocyanuric Acid

Bárbara V. Silva,* Pierre M. Esteves and Angelo C. Pinto

Instituto de Química-CT, Universidade Federal do Rio de Janeiro, Cidade Universitária, 21945-970 Rio de Janeiro-RJ, Brazil

Synthesis and characterization of the chloroisatins

Typical procedure for the reaction in HOAc

To a suspension of TCCA and HOAc the isatin derivative was added. The reaction medium was kept stirring at different temperatures and times (Tables 1 and 2). The mixture was then poured over cracked ice. The precipitate was filtered under vacuum and washed thoroughly with water. Subsequently, the product was solubilized in ethyl acetate, filtered and the solution evaporated at reduced pressure to separate the isocyanuric acid formed as byproduct.

Typical procedure for the reaction in H_2SO_4

To a suspension of TCCA and H_2SO_4 was added the isatin derivative in an ice bath. After the complete addition of the isatin, the ice bath was removed, and the mixture was kept stirring during the time described in Table 3. The mixture was then poured over cracked ice. The precipitate was filtered under vacuum and washed thoroughly with water. Subsequently, the product was solubilized in ethyl acetate, filtered and the solution evaporated at reduced pressure to separate the isocyanuric acid formed as byproduct. The products (**9b**) and (**9c**) were separated by high performance liquid chromatography (HPLC) and analyzed separately by ^{1}H and ^{13}C NMR.

Separation by HPLC

Separation by HPLC of (**9b**) and (**9c**) was performed on Agilent 1100 series chromatograph detection by ultraviolet (UV, λ_{max}/nm 280). Semi-preparative method in a reversed phase column C-18 (Agilent Zorbax Eclipse, 9.4 mm (diameter) × 250 mm (length), 5 micron) under isocratic conditions using 45% water and 55% methanol as mobile phase, flow 3 mL/min, with 30 min elution was employed.

*e-mail: barbara.iq@gmail.com

Computational details

All calculations were carried out with the Gaussian 09 package[1] using the M06-2X functional with the 6-311++G** basis set. The optimized geometries were characterized as minima on the potential energy surface by the absence of imaginary vibrational frequencies. All energy differences correspond to enthalpies differences at 298K and 1 atm.

Spectroscopic data

1a: IR (film) ν_{max}/cm^{-1}: 3085, 2923, 1764, 1729, 1614, 1596, 1483, 1315, 1294, 1176, 1126, 950, 427. ^{1}H NMR δ (200 MHz, $CDCl_3$): 3.23 (3H, s), 6.85 (1H, d, *J* 8.0 Hz), 7.51-7.57 (2H, m); ^{13}C NMR δ (50 MHz, $CDCl_3$): 26.5 (CH_3), 111.4 (CH), 118.3 (q), 125.2 (CH), 129.7 (q), 137.9 (CH), 149.8 (q), 157.8 (q), 182.4 (q); MS (70 eV) *m/z* 195 $[M]^+$, 197 $[M+2]^+$, 160, 104.

2a: IR (film) ν_{max}/cm^{-1}: 3060, 1770, 1743, 1606, 1456, 1423, 1307, 1270, 1178, 1160, 827, 717, 466. ^{1}H NMR δ (200 MHz, $CDCl_3$): 7.07 (1H, d, *J* 8.0 Hz), 7.71 (1H, d, *J* 2.0 Hz), 7.81 (1H, dd, *J* 2.0 and 8.0 Hz); ^{13}C NMR δ (50 MHz, $CDCl_3$): 113.0 (CH), 118.0 (q), 120.5 (q), 127.9 (CH), 141.2

1. Frisch, M. J.; Trucks, G. W.; Schlegel, H. B.; Scuseria, G. E.; Robb, M. A.; Cheeseman, J. R.; Scalmani, G.; Barone, V.; Mennucci, B.; Petersson, G. A.; Nakatsuji, H.; Caricato, M.; Li, X.; Hratchian, H. P.; Izmaylov, A. F.; Bloino, J.; Zheng, G.; Sonnenberg, J. L.; Hada, M.; Ehara, M.; Toyota, K.; Fukuda, R.; Hasegawa, J.; Ishida, M.; Nakajima, T.; Honda, Y.; Kitao, O.; Nakai, H.; Vreven, T.; Montgomery, Jr., J. A.; Peralta, J. E.; Ogliaro, F.; Bearpark, M.; Heyd, J. J.; Brothers, E.; Kudin, K. N.; Staroverov, V. N.; Kobayashi, R.; Normand, J.; Raghavachari, K.; Rendell, A.; Burant, J. C.; Iyengar, S. S.; Tomasi, J.; Cossi, M.; Rega, N.; Millam, N. J.; Klene, M.; Knox, J. E.; Cross, J. B.; Bakken, V.; Adamo, C.; Jaramillo, J.; Gomperts, R.; Stratmann, R. E.; Yazyev, O.; Austin, A. J.; Cammi, R.; Pomelli, C.; Ochterski, J. W.; Martin, R. L.; Morokuma, K.; Zakrzewski, V. G.; Voth, G. A.; Salvador, P.; Dannenberg, J. J.; Dapprich, S.; Daniels, A. D.; Farkas, O.; Foresman, J. B.; Ortiz, J. V.; Cioslowski, J.; Fox, D. J.; *Gaussian 03, Revision C.02*, Gaussian, Inc.: Wallingford CT, 2004.

(CH), 148.0 (q), 154.7 (q), 176.8 (q), 182.4 (q); MS (70 eV) *m/z* 259 $[M]^+$, 261, $[M+2]^+$, 263 $[M+3]^+$, 168, 226.

2b: IR (film) ν_{max}/cm^{-1}: 3471, 3174, 3110, 1754, 1610, 1457, 1425, 1290, 1224, 1168, 837; ^1H NMR δ (200 MHz, $CDCl_3$+DMSO): 7.47 (1H, s), 7.58 (1H, s), 11.43 (1H, br s, NH); ^{13}C NMR δ (50 MHz, $CDCl_3$+DMSO): 114.8 (q), 118.2 (q), 119.5 (q), 125.5 (CH), 139.1 (CH), 146.8 (q), 158.3 (q), 182.1 (q); MS (70 eV) *m/z* 259 $[M]^+$, 261, $[M+2]^+$, 263 $[M+3]^+$, 233, 205.

5b: IR (film) ν_{max}/cm^{-1}: 3467, 3423, 1751, 1727, 1608, 1457, 1467, 1326, 1176, 1108, 827; ^1H NMR δ (200 MHz, $CDCl_3$+DMSO): 3.16 (3H, s), 6.89 (1H, d, *J* 8.0 Hz), 7.43 (1H, s), 7.52 (1H, d, *J* 8.0 Hz), 11.43 (1H, br s, NH); ^{13}C NMR δ (50 MHz, $CDCl_3$+DMSO): 25.4 (CH_3), 116.6 (CH), 123.1 (q), 129.5 (CH), 134.0 (q), 142.6 (CH), 154.6 (q), 162.6 (q), 187.3 (q); MS (70 eV) *m/z* 195 $[M]^+$, 197 $[M+2]^+$, 167, 139.

6b: IR (film) ν_{max}/cm^{-1}: 3452, 3415, 3178, 3102, 1743, 1616, 1469, 1297, 889, 700; ^1H NMR δ (200 MHz, $CDCl_3$+DMSO): 2.15 (3H, s), 7.20 (1H, br s), 7.27 (1H, br s), 11.13 (1H, br s, NH); ^{13}C NMR δ (50 MHz, $CDCl_3$+DMSO): 14.2 (CH_3), 117.0 (q), 120.3 (CH), 122.8 (q), 126.3 (CH), 137.2 (CH), 146.9 (q), 158.3 (q), 182.6 (q); MS (70 eV) *m/z* 195 $[M]^+$, 197 $[M+2]^+$, 167, 139, 104.

7b: IR (film) ν_{max}/cm^{-1}: 3488, 3473, 3180, 3114, 1743, 1754, 1621, 1600, 1479, 1299, 1211, 1099, 925, 867, 796; ^1H NMR δ (200 MHz, $CDCl_3$+DMSO): 6.92 (1H, d *J* 7.0 Hz), 7.04 (1H, d *J* 7.0 Hz), 11.04 (1H, br s, NH); ^{13}C NMR δ (50 MHz, $CDCl_3$+DMSO): 110.1 (CH_2 d *J* 27 Hz), 117.7 (q, d *J* 7.0 Hz), 118.6 (q, d, *J* 7.0 Hz) 124.4 (CH, d, *J* 27 Hz), 144.3 (q, d, *J* 2.5 Hz), 157.7 (q, d, *J* 246.5 Hz), 158.9 (q), 182.8 (q, d *J* 2.5 Hz). MS (70 eV) *m/z* 199 $[M]^+$, 201 $[M+2]^+$, 171, 143.

9c: IR (film) ν_{max}/cm^{-1}: 3193, 3182, 3099, 1770, 1745, 1610, 1450, 1164, 983, 688; ^1H NMR δ (200 MHz, $CDCl_3$+DMSO): 7.71 (1H, d *J* 1.5 Hz), 7.77 (1H, d *J* 1.5 Hz), 10.78 (1H, br s, NH); ^{13}C NMR δ (50 MHz, $CDCl_3$+DMSO): 84.79 (q), 118.97 (q), 120.36 (q), 132.03 (CH), 145.34 (CH), 147.48 (q), 158.23 (q), 182.14 (q); MS (70 eV) *m/z* 307 $[M]^+$, 309 $[M+2]^+$, 279, 251.

11b: IR (film) ν_{max}/cm^{-1}: 3479, 3465, 3268, 3087, 1766, 1791, 1594, 1558, 1388, 1247, 958; ^1H NMR δ (200 MHz, $CDCl_3$+DMSO): 6.29 (1H, s), 10.40 (1H, br s, NH); ^{13}C NMR δ (50 MHz, $CDCl_3$+DMSO): 114.3 (CH), 118.7 (q), 126.3 (q), 127.8 (q), 129.5 (q), 148.6 (q), 156.4 (q), 178.5 (q); MS (70 eV) *m/z* 337 $[M]^+$, 339 $[M+2]^+$, 341 $[M+3]^+$, 343 $[M+4]^+$, 311, 284, 204.

^1H and ^{13}C NMR spectra

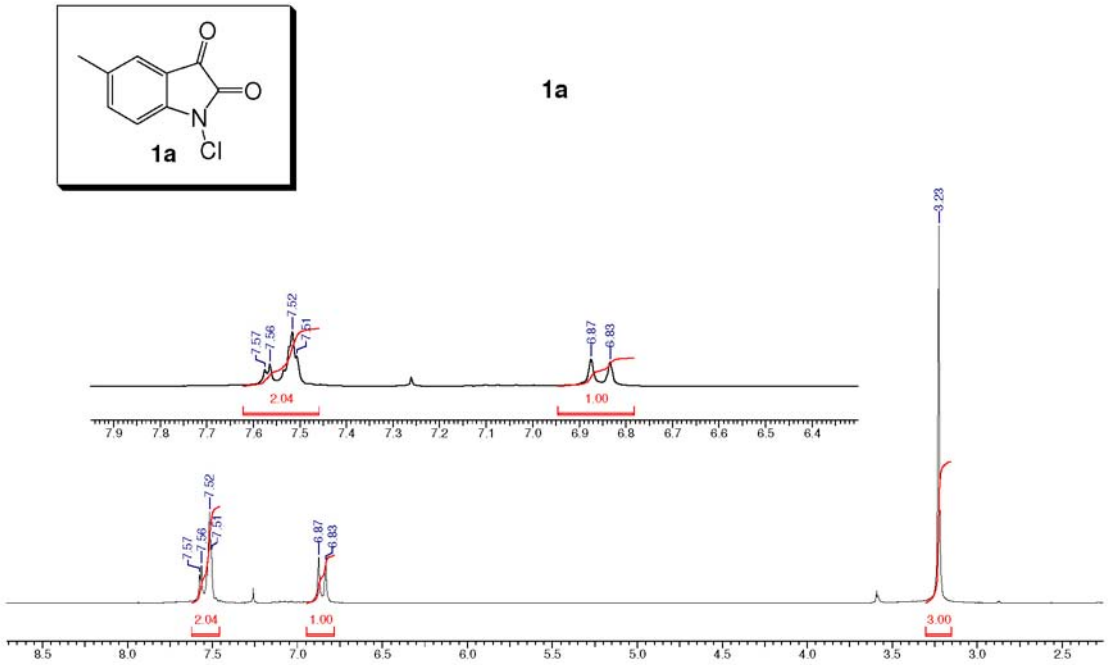

Figure S1. ^1H NMR of **1a**.

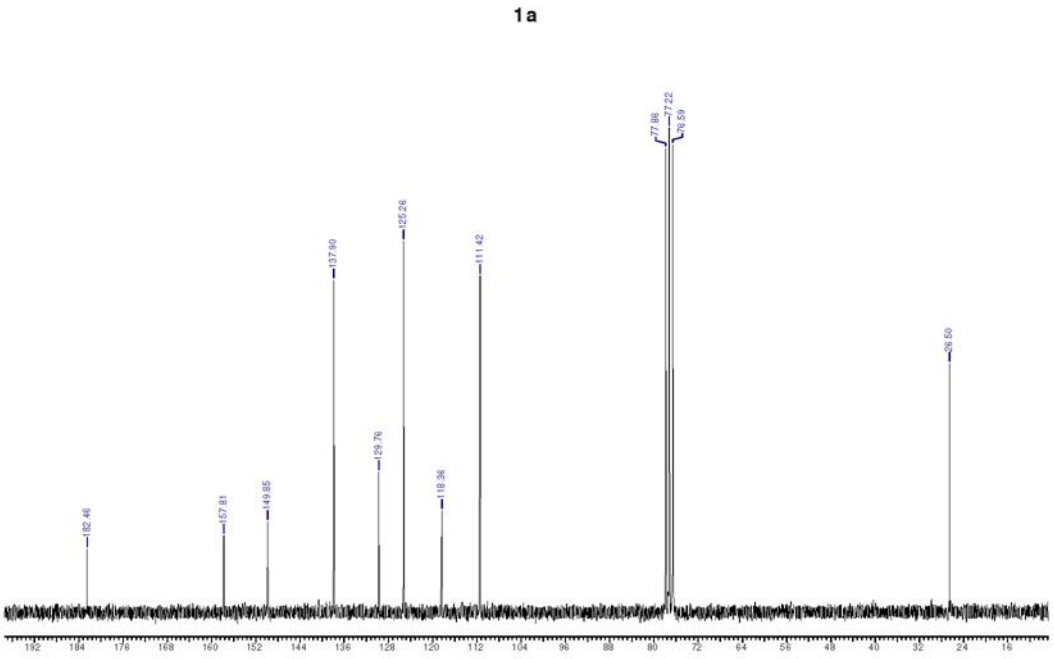

Figure S2. ^{13}C NMR of **1a**.

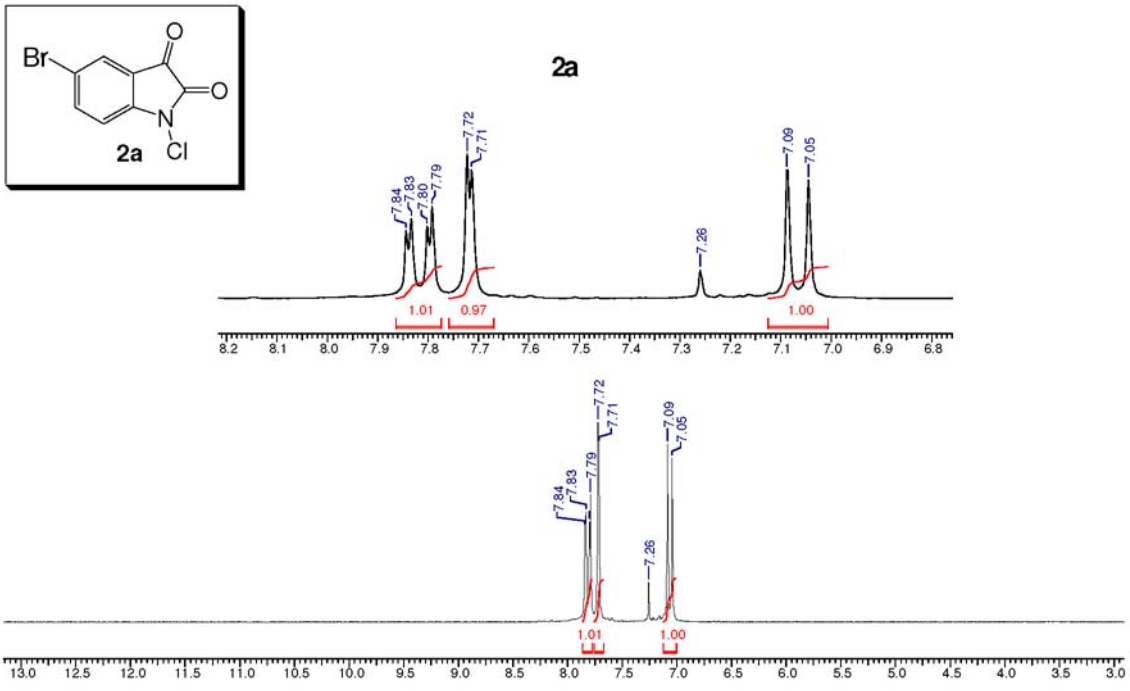

Figure S3. ^{1}H NMR of **2a**.

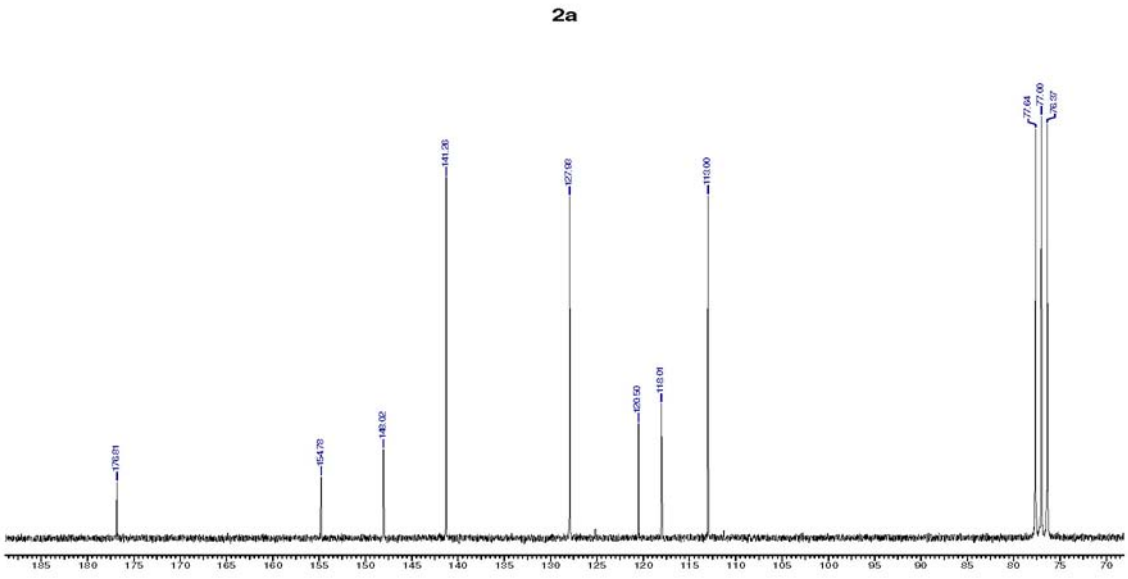

Figure S4. ^{13}C NMR of **2a**.

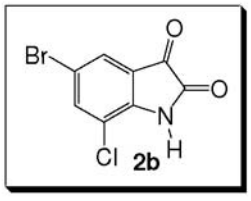

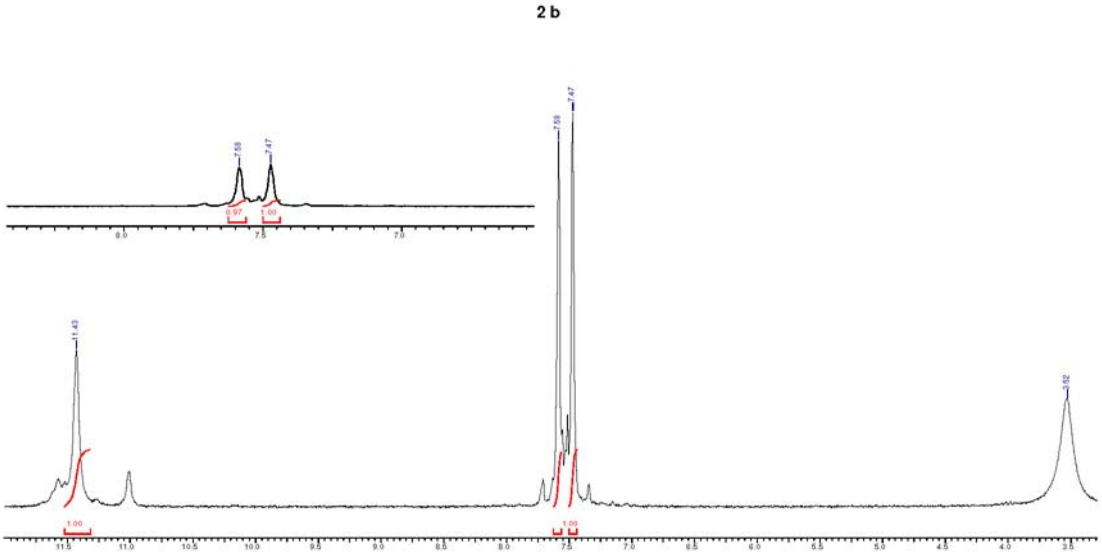

Figure S5. ^{1}H NMR of **2b**.

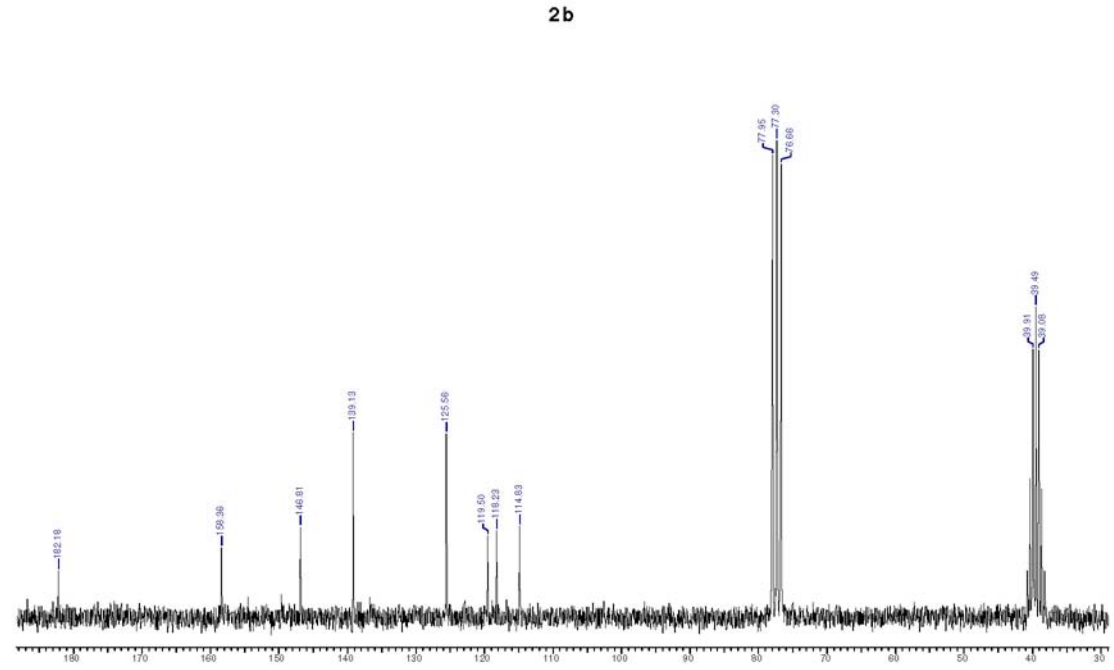

Figure S6. ^{13}C NMR of **2b**.

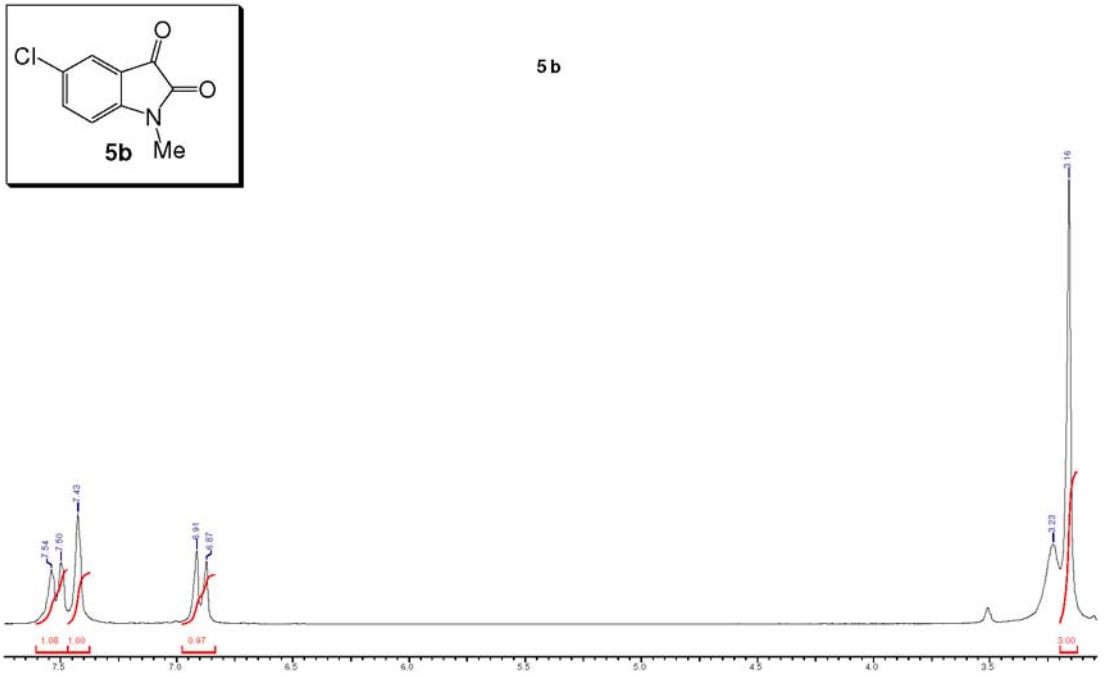

Figure S7. ^{1}H NMR of **5b**.

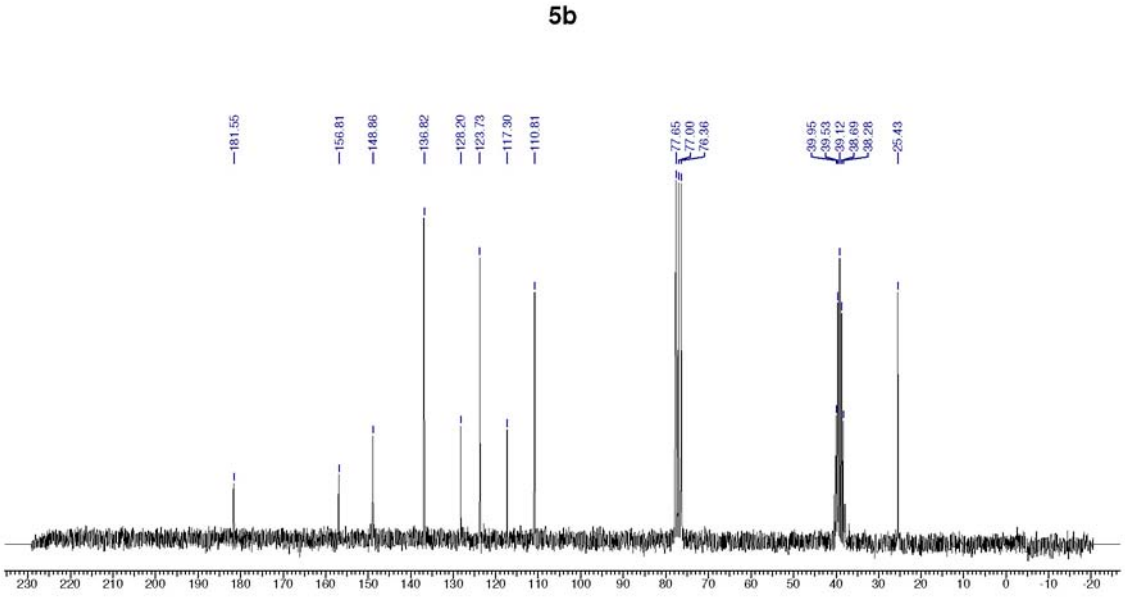

Figure S8. ^{13}C NMR of **5b**.

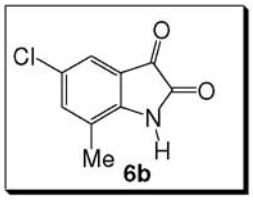

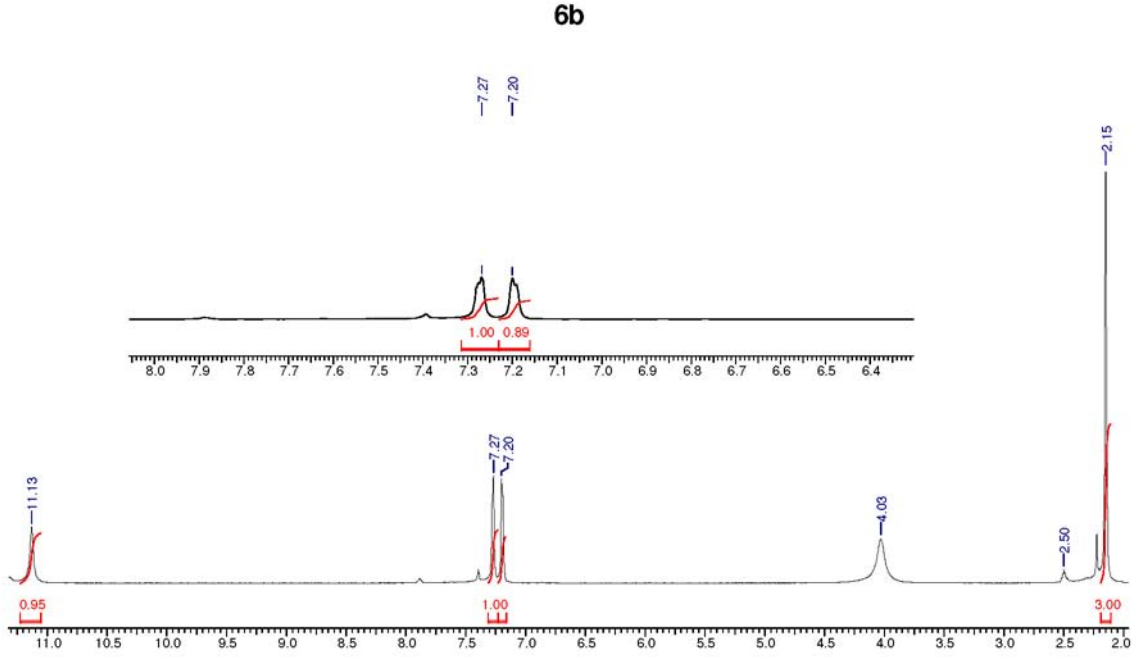

Figure S9. ^{1}H NMR of **6b**.

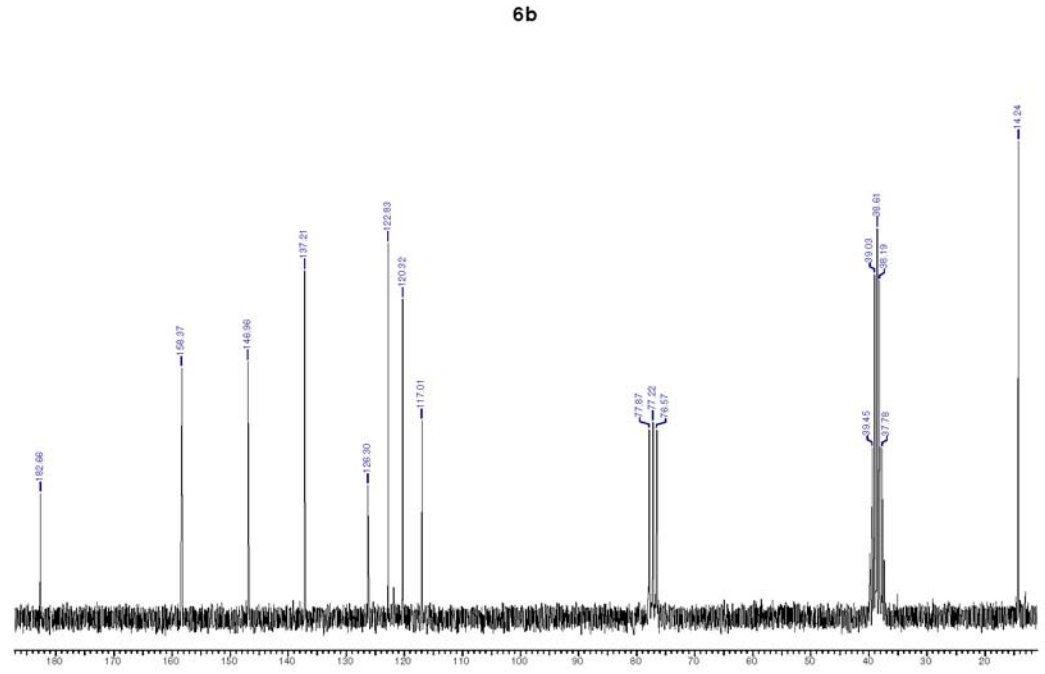

Figure S10. ^{13}C NMR of **6b**.

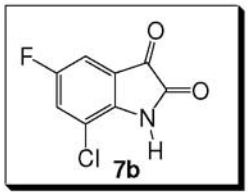

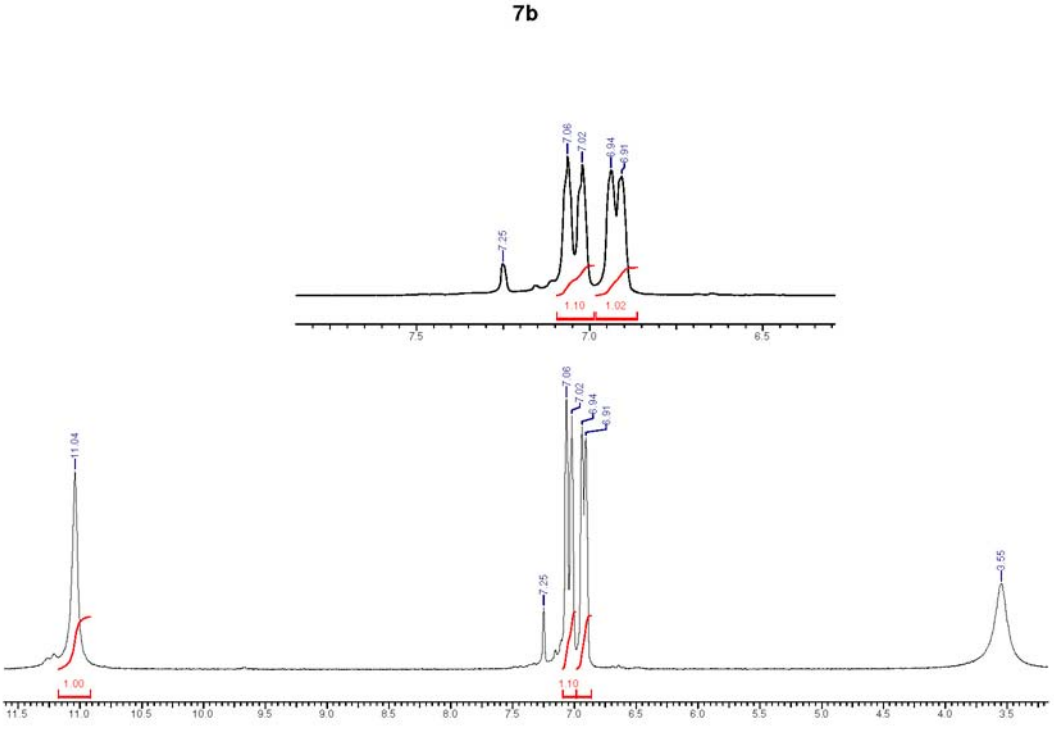

Figure S11. ^{1}H NMR of **7b**.

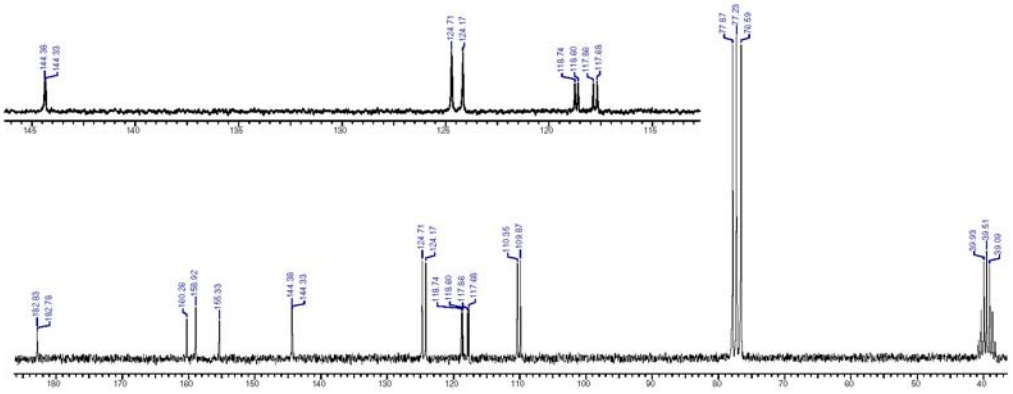

Figure S12. ^{13}C NMR of **7b**.

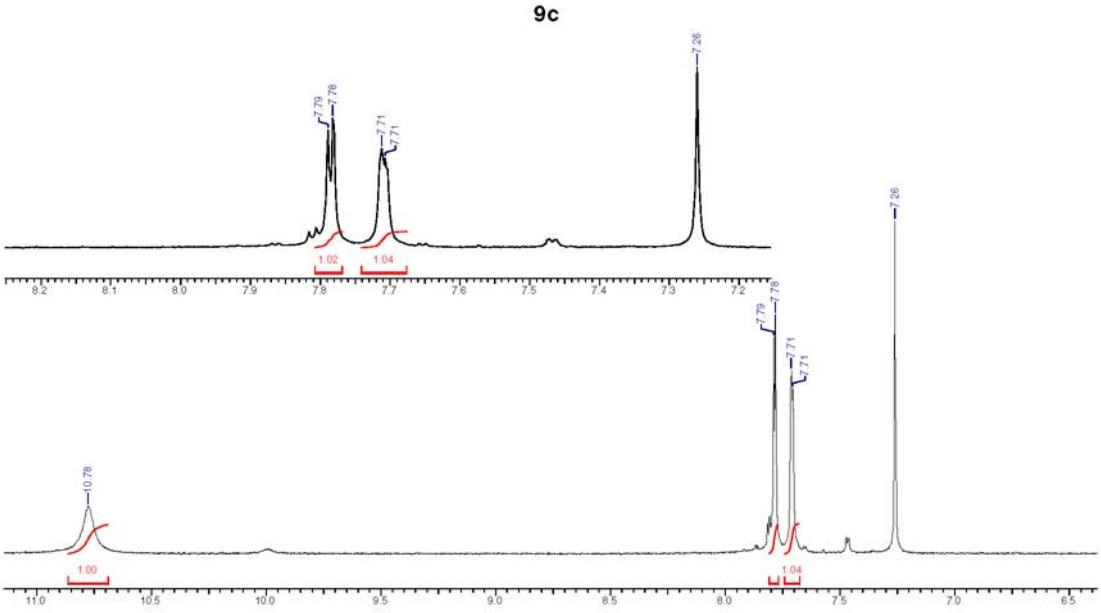

Figure S13. ^{1}H NMR of **9c**.

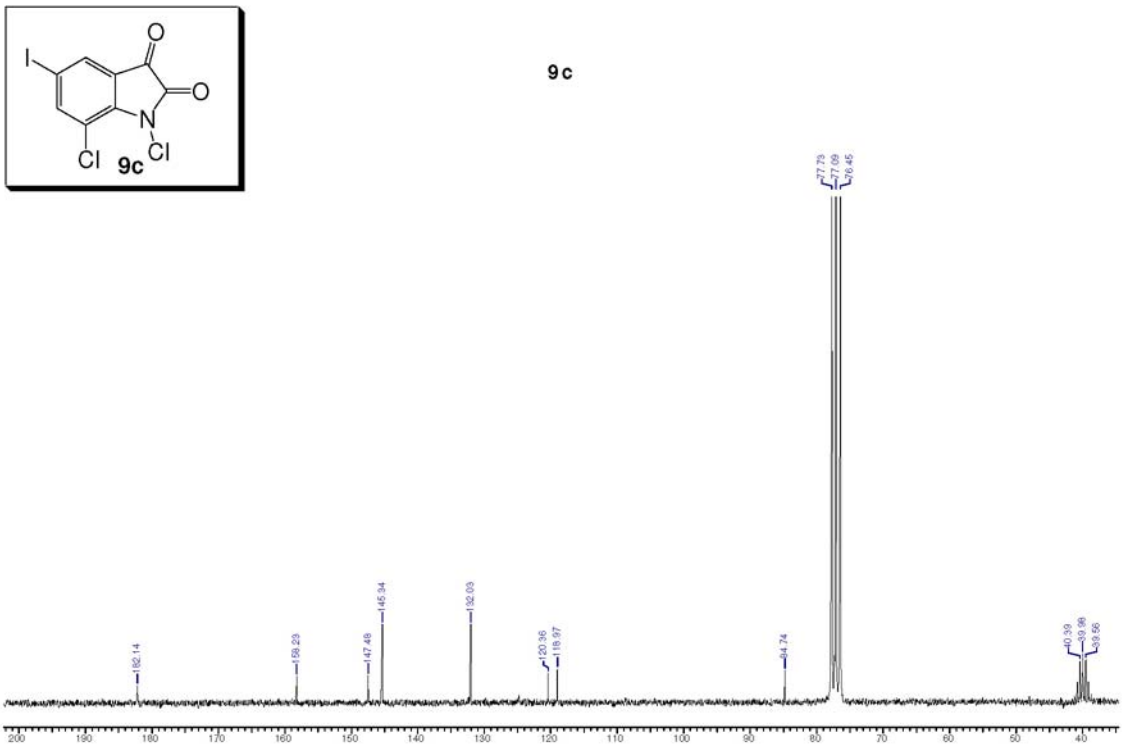

Figure S14. [13]C NMR of **9c**.

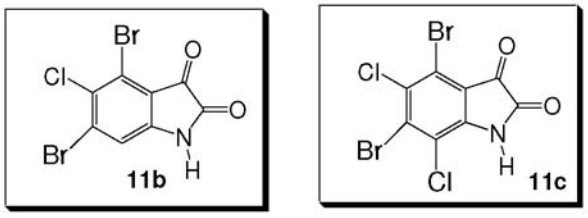

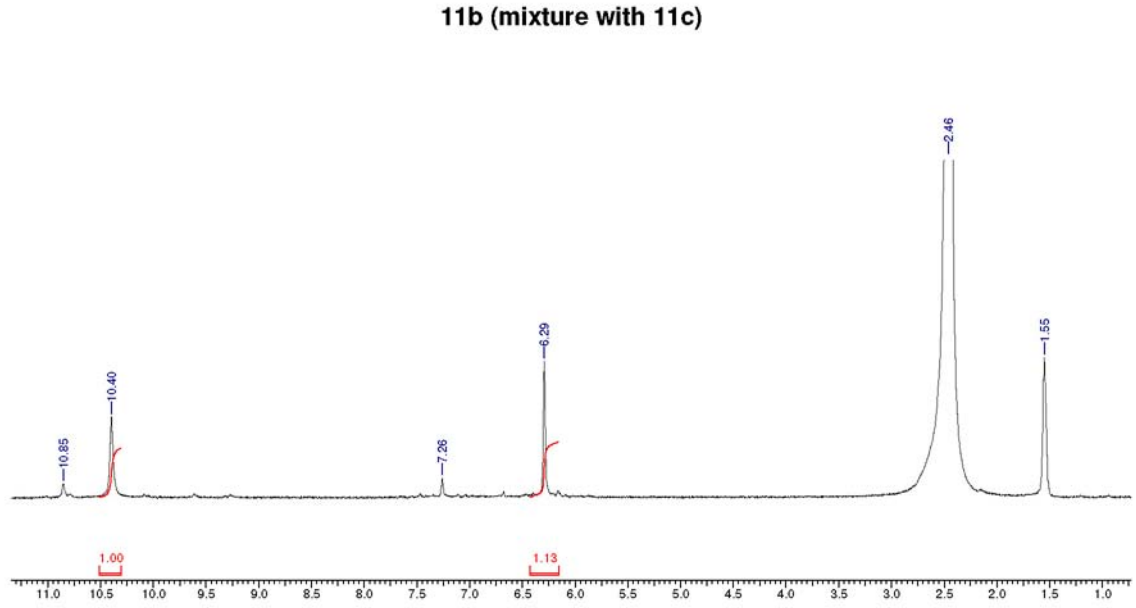

Figure S15. [1]H NMR of **11b** (mixture with **11c**).

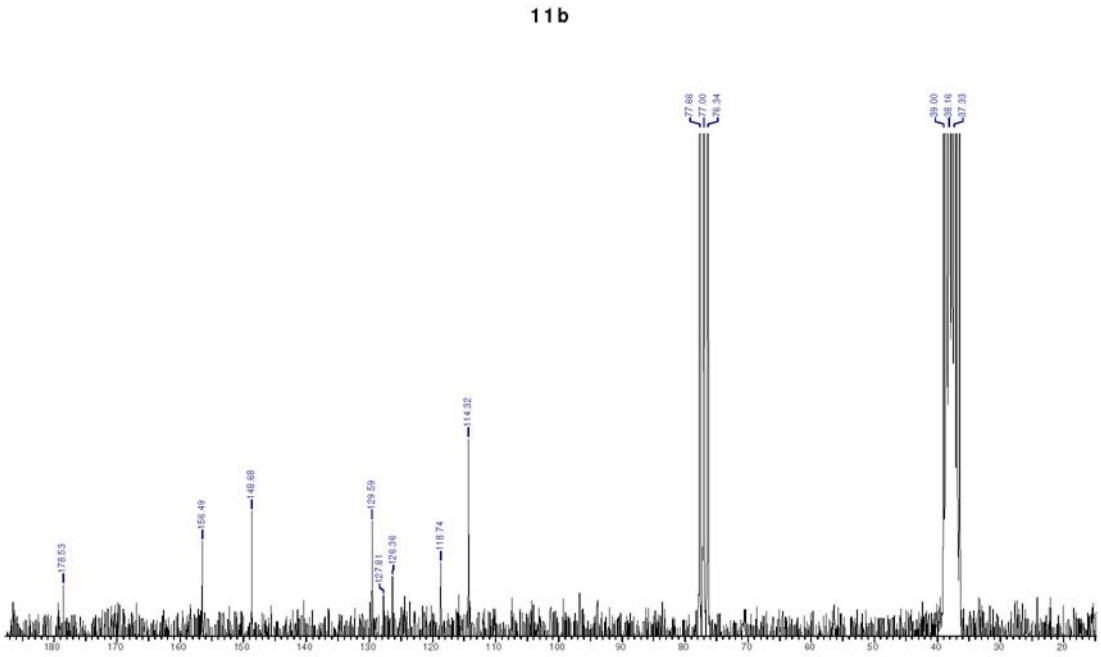

Figure S16. ^{13}C NMR of **11b**.

FTIR spectra

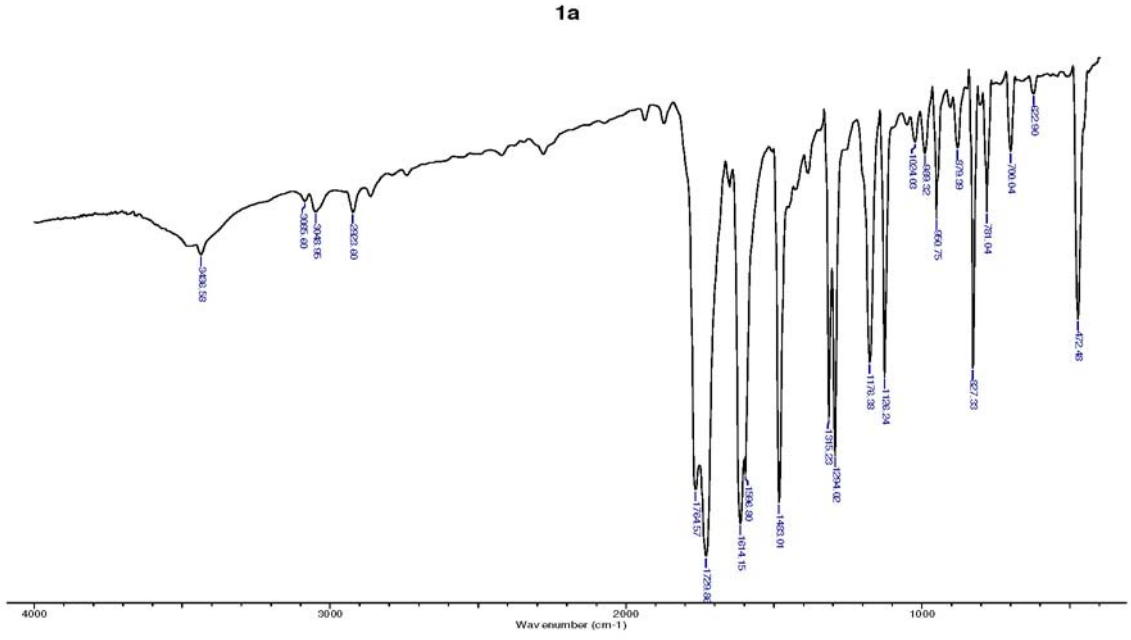

Figure S17. FTIR spectra of **1a**.

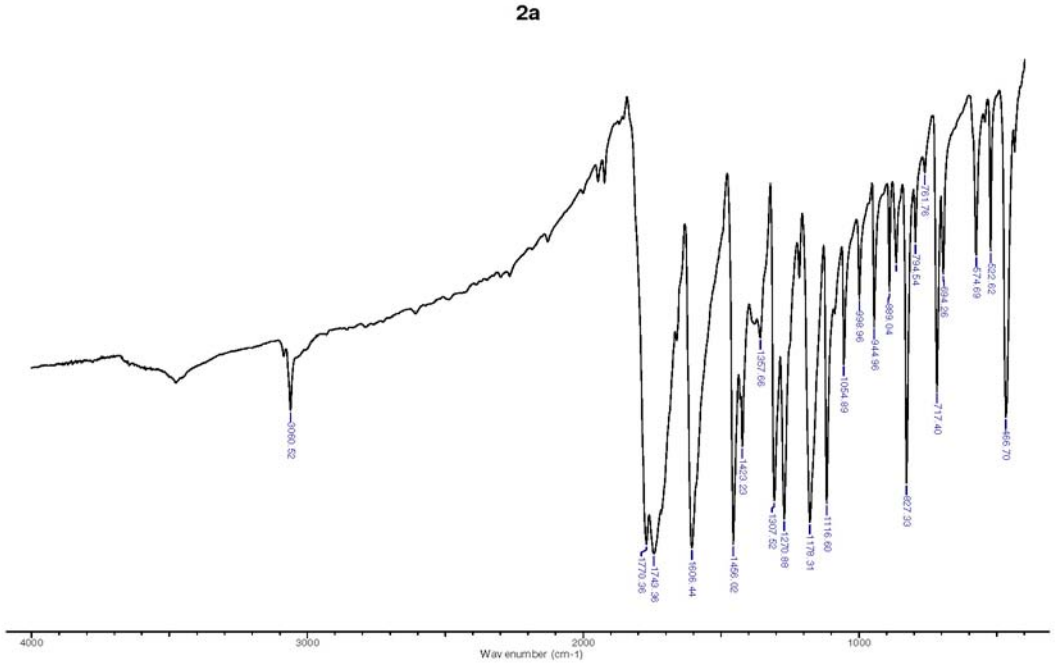

Figure S18. FTIR spectra of **2a**.

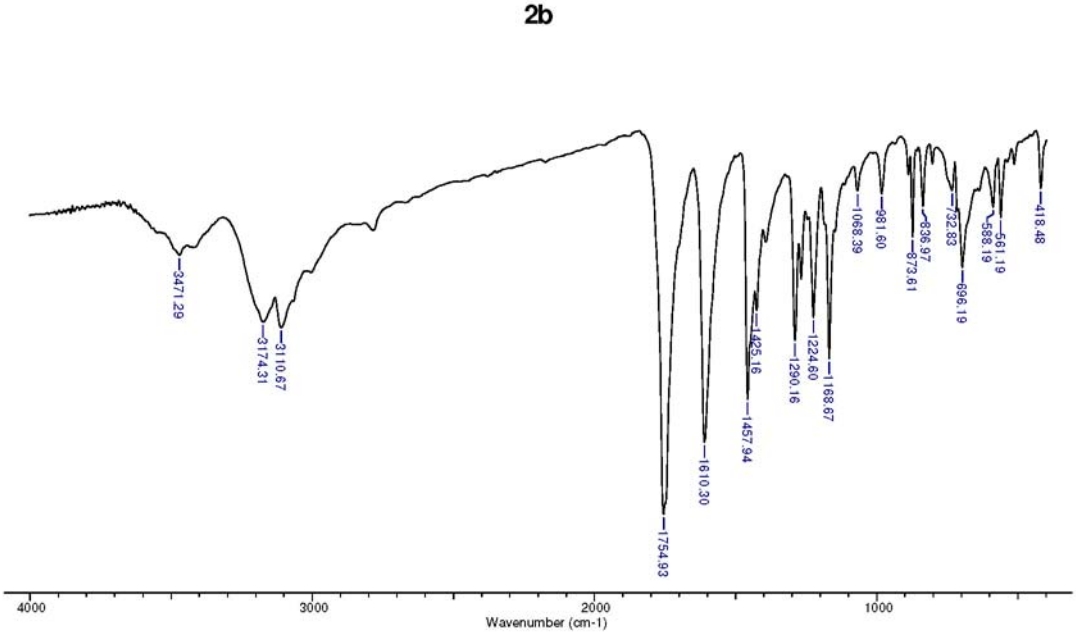

Figure S19. FTIR spectra of **2b**.

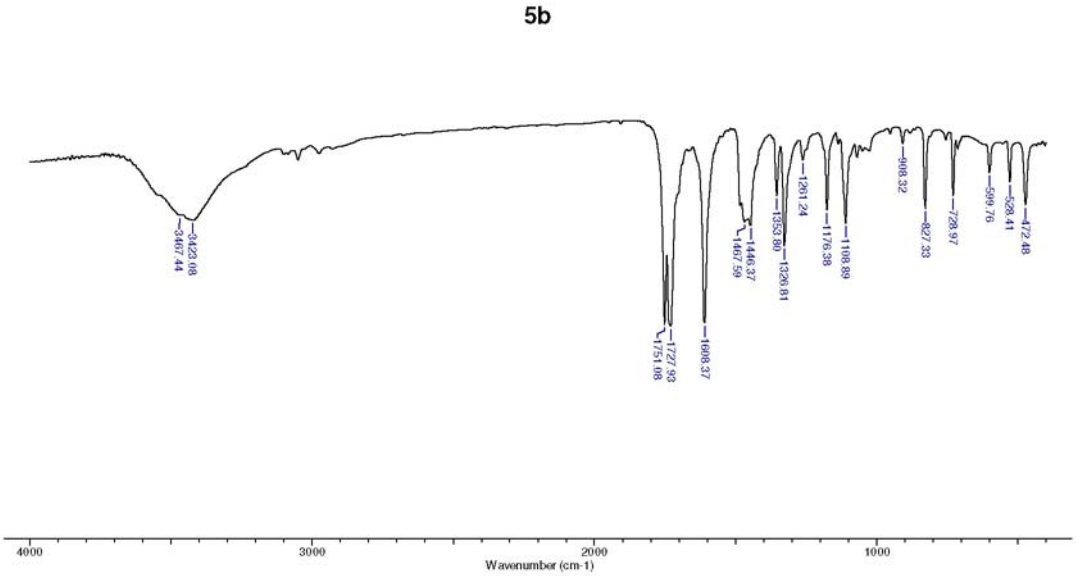

Figure S20. FTIR spectra of **5b**.

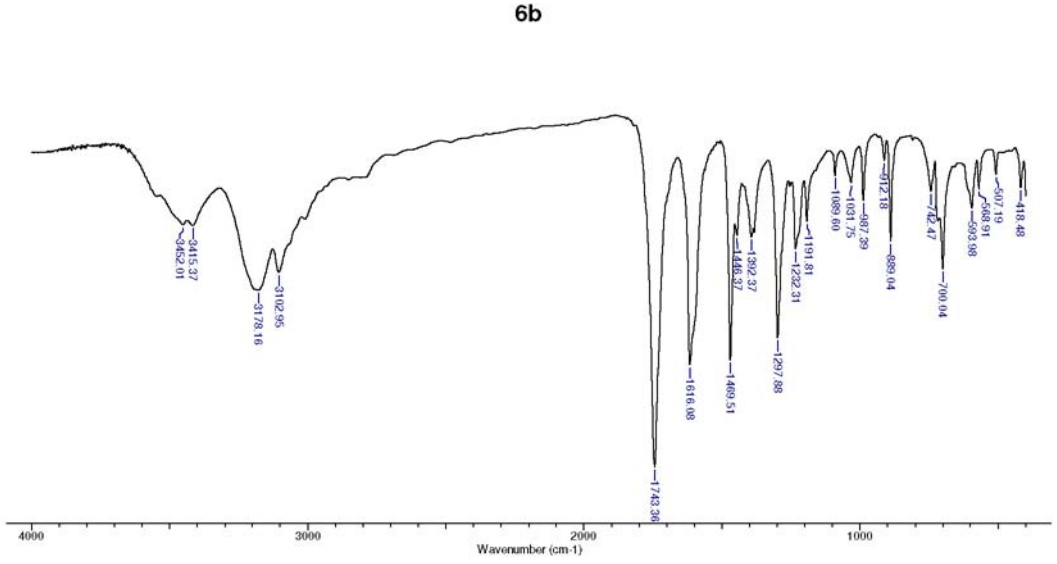

Figure S21. FTIR spectra of **6b**.

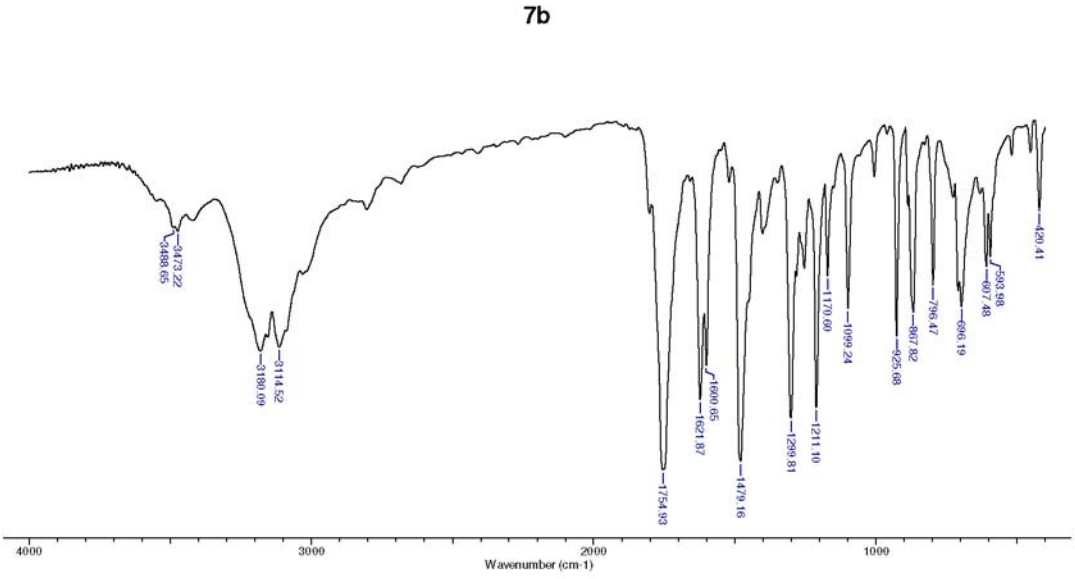

Figure S22. FTIR spectra of **7b**.

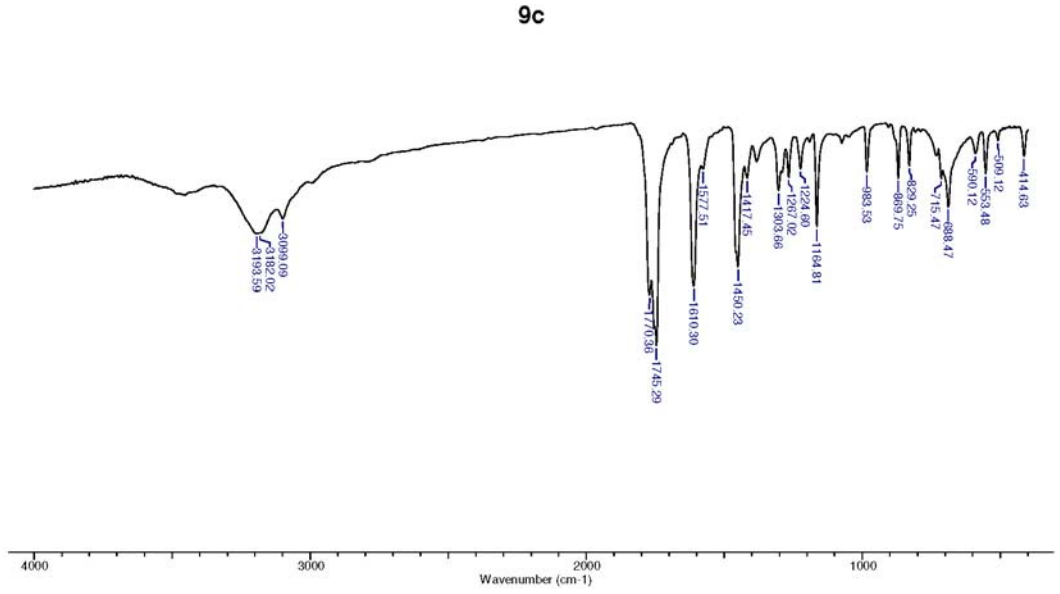

Figure S23. FTIR spectra of **9c**.

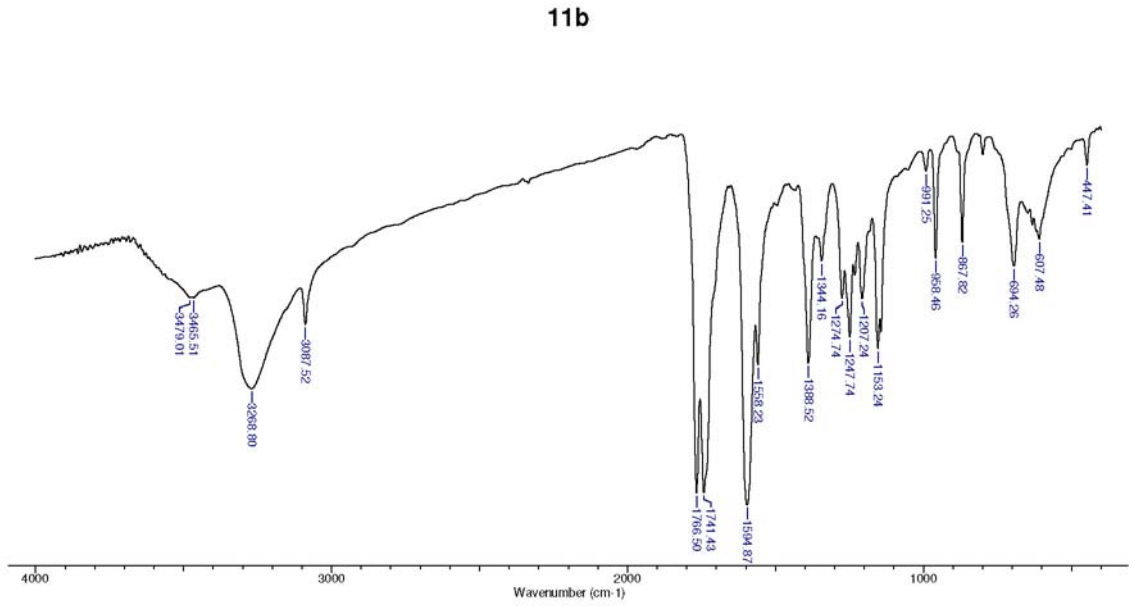

Figure S24. FTIR spectra of **11b.**

Mass Spectra

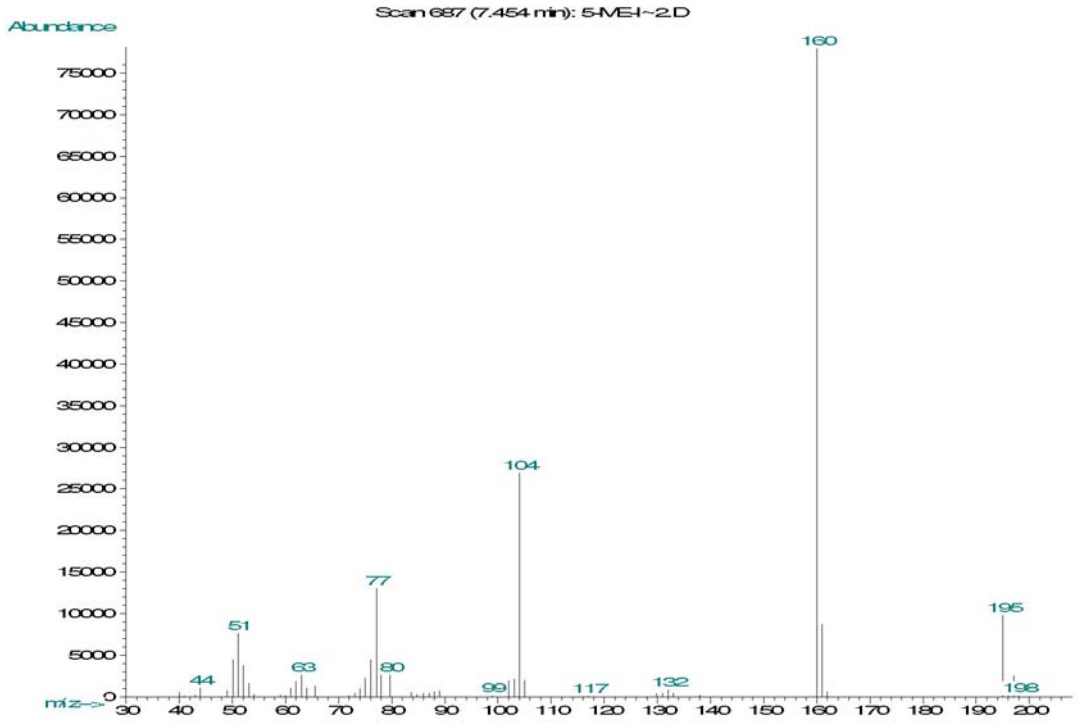

Figure S25. Mass spectrum of **1a**.

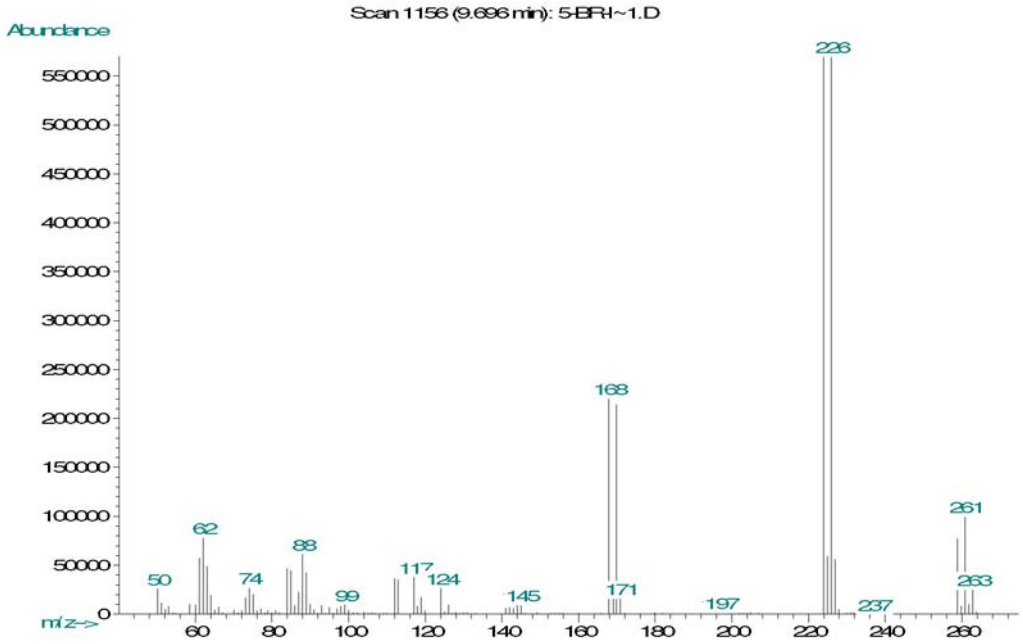

Figure S26. Mass spectrum of **2a**.

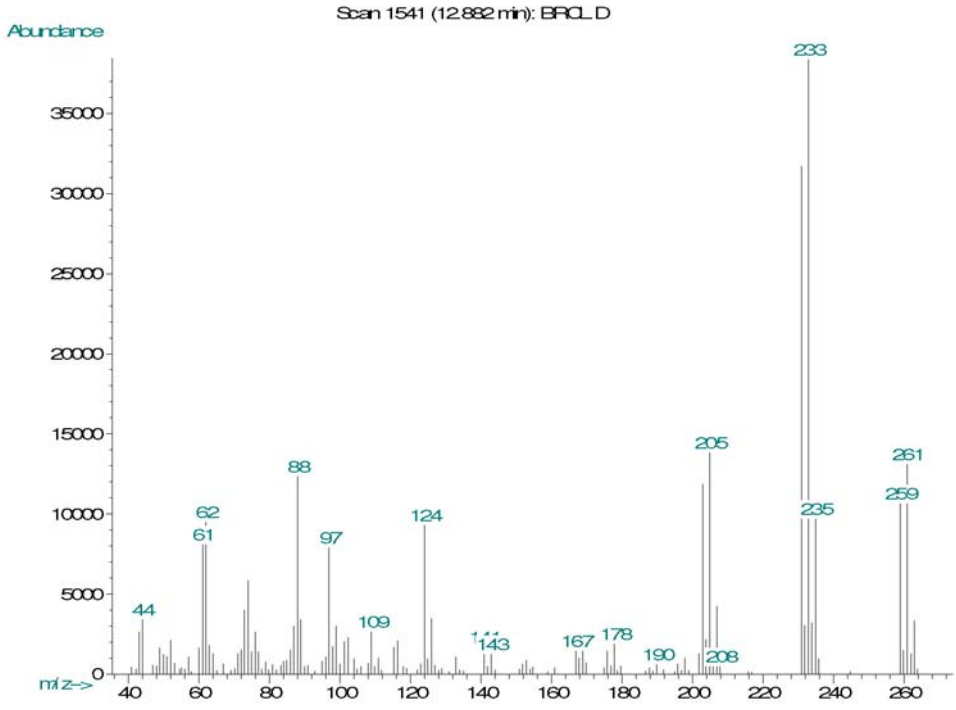

Figure S27. Mass spectrum of **2b**.

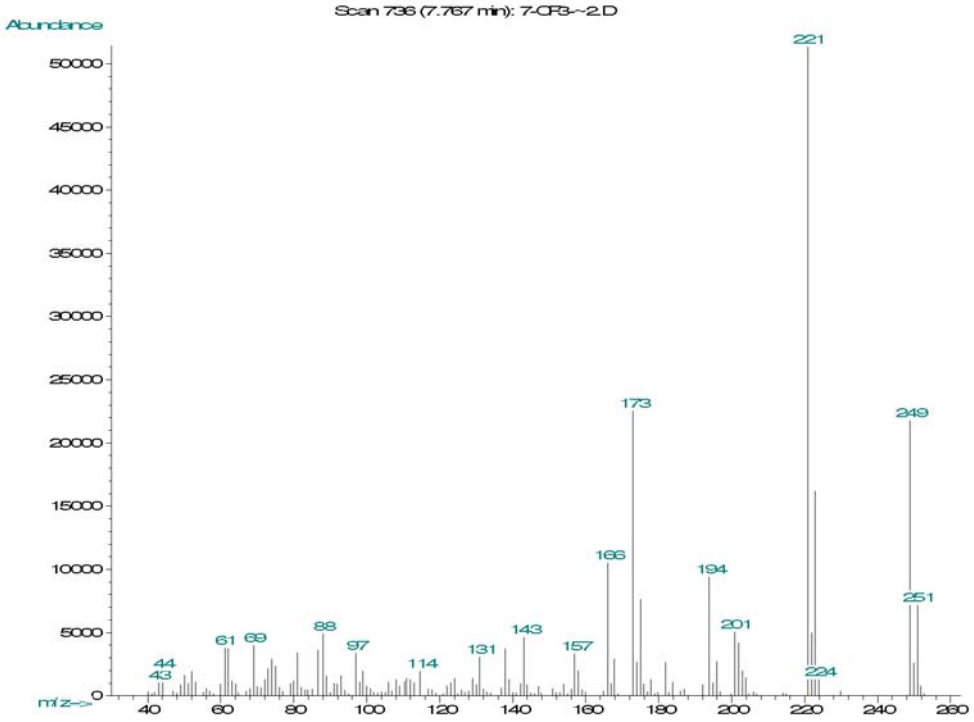

Figure S28. Mass spectrum of **4b**.

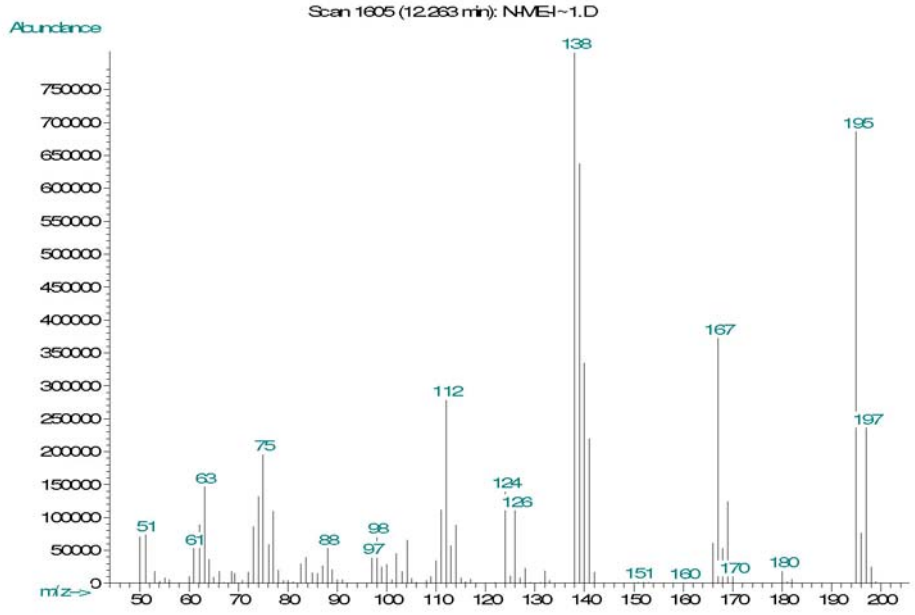

Figure S29. Mass spectrum of **5b**.

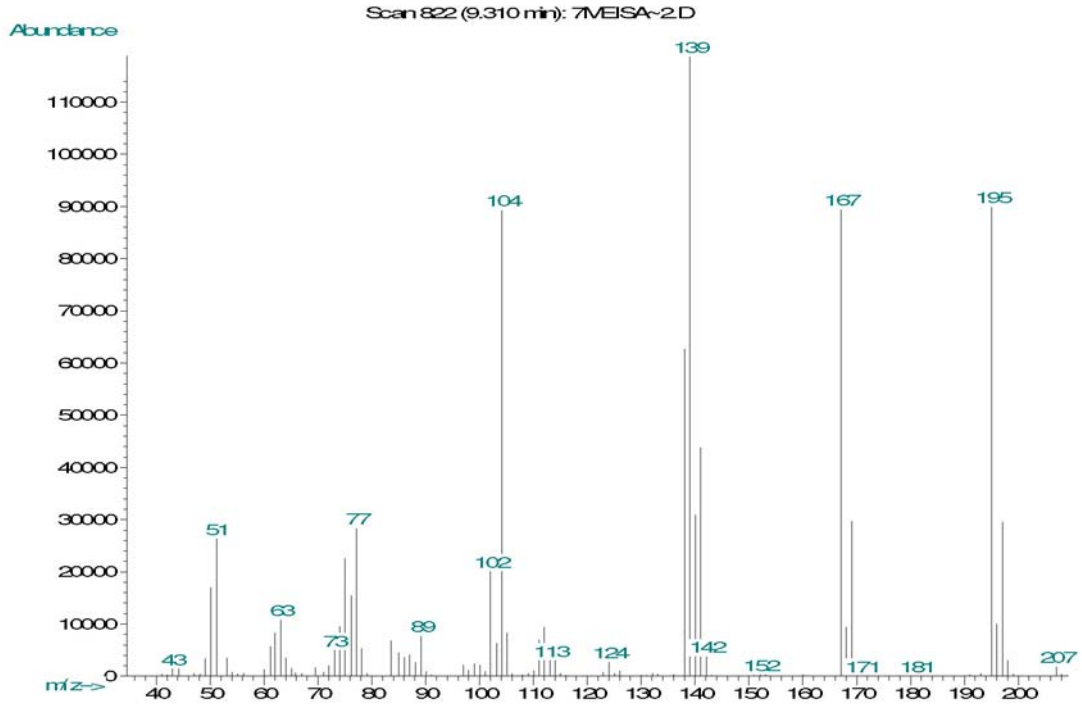

Figure S30. Mass spectrum of **6b**.

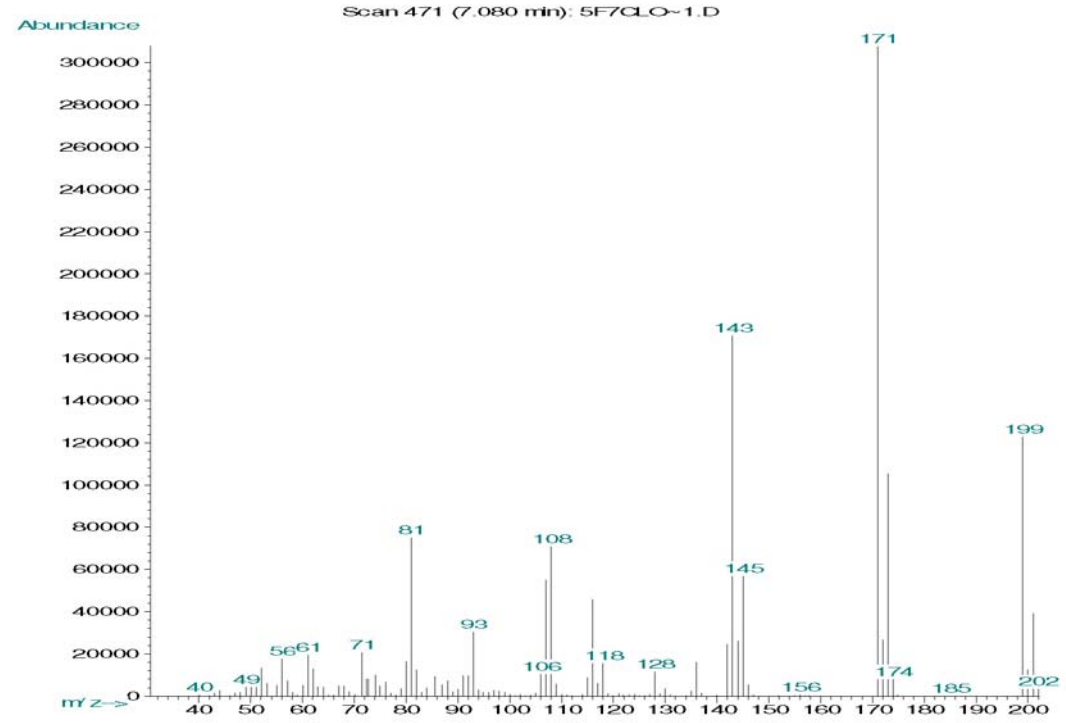

Figure S31. Mass spectrum of **7b**.

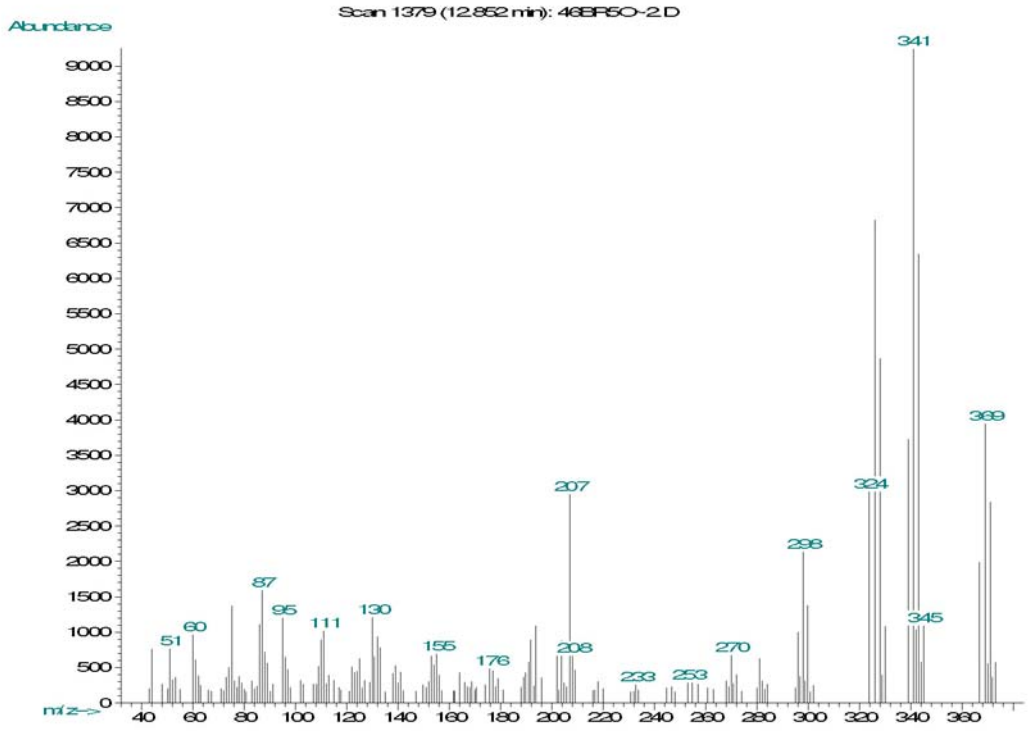

Figure S32. Mass spectrum of **8b**.

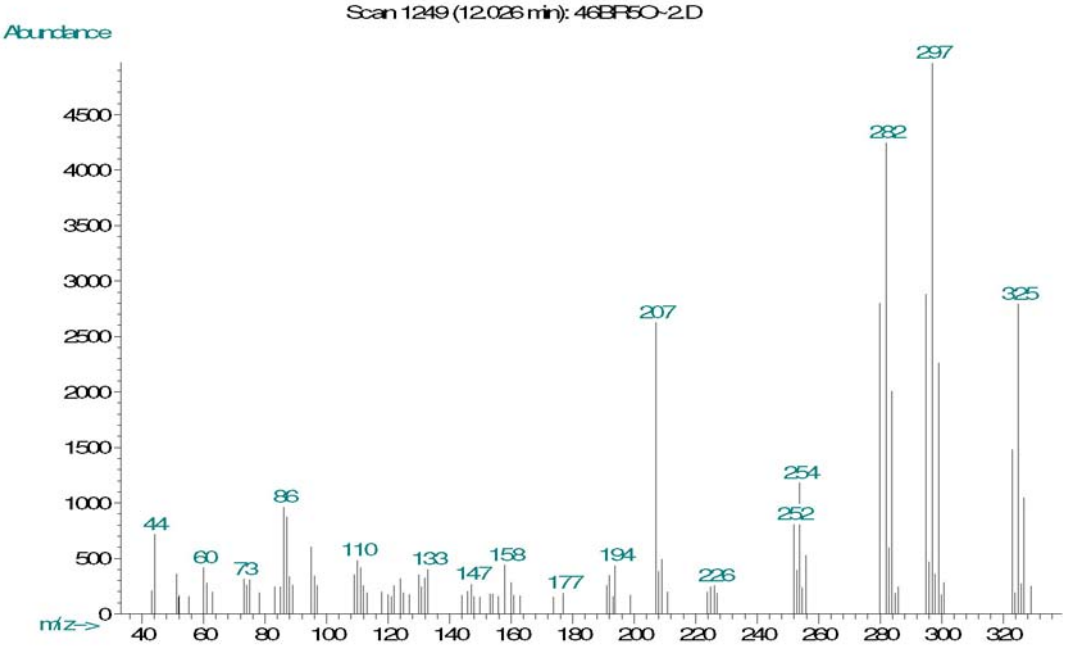

Figure S33. Mass spectrum of **8c**.

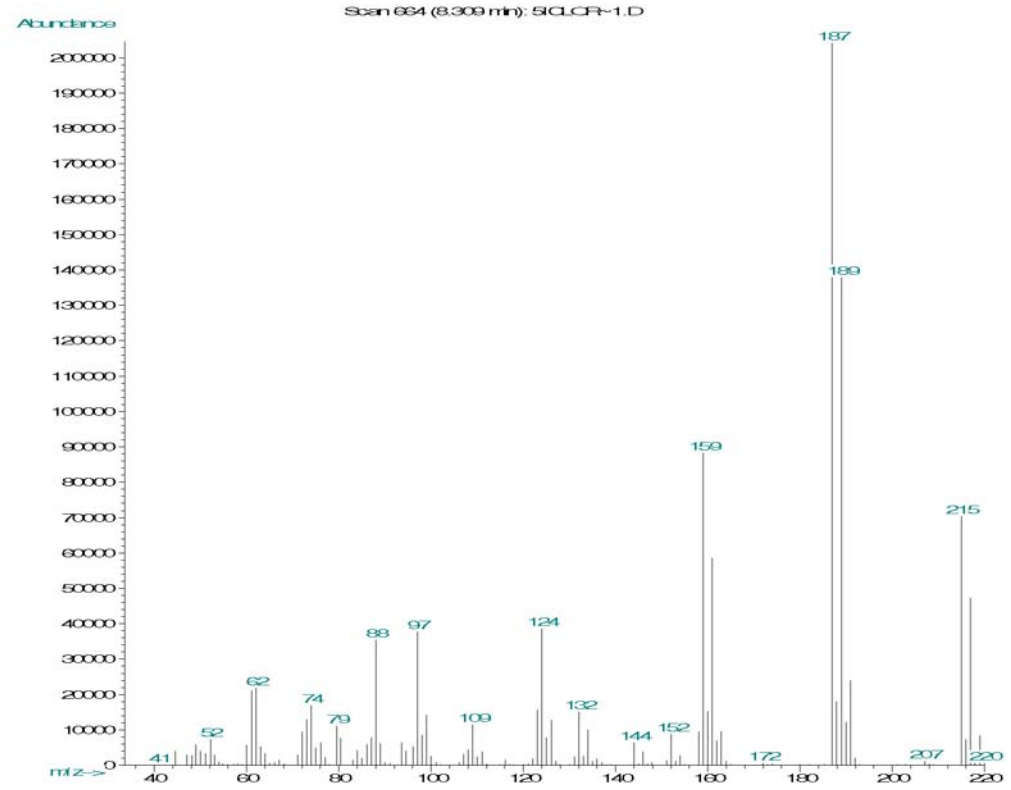

Figure S34. Mass spectrum of **9b**.

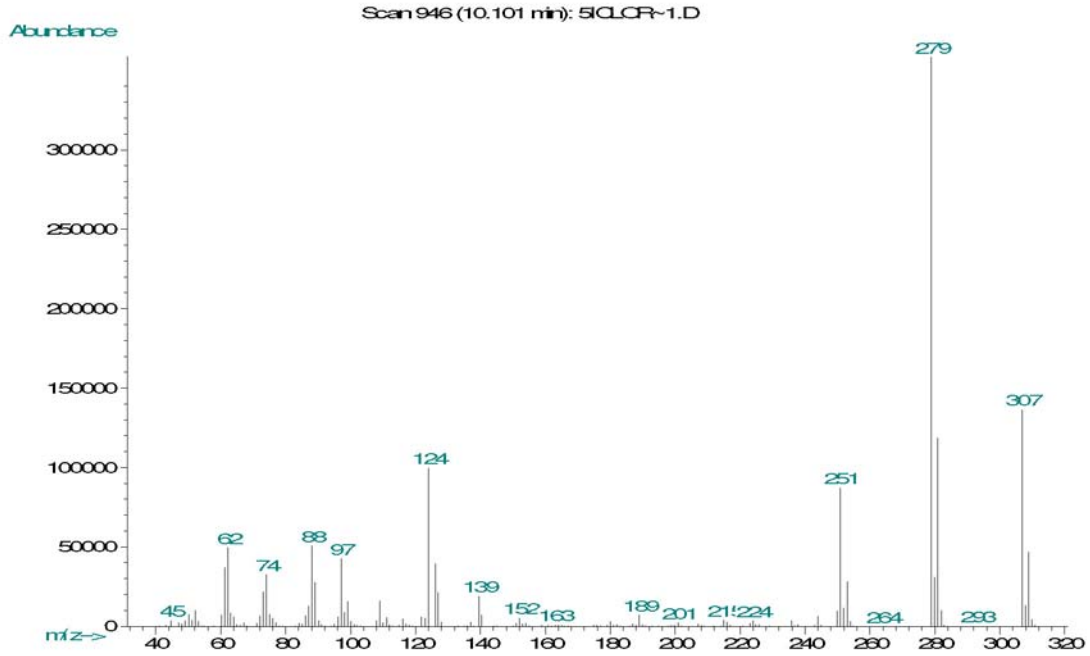

Figure S35. Mass spectrum of **9c**.

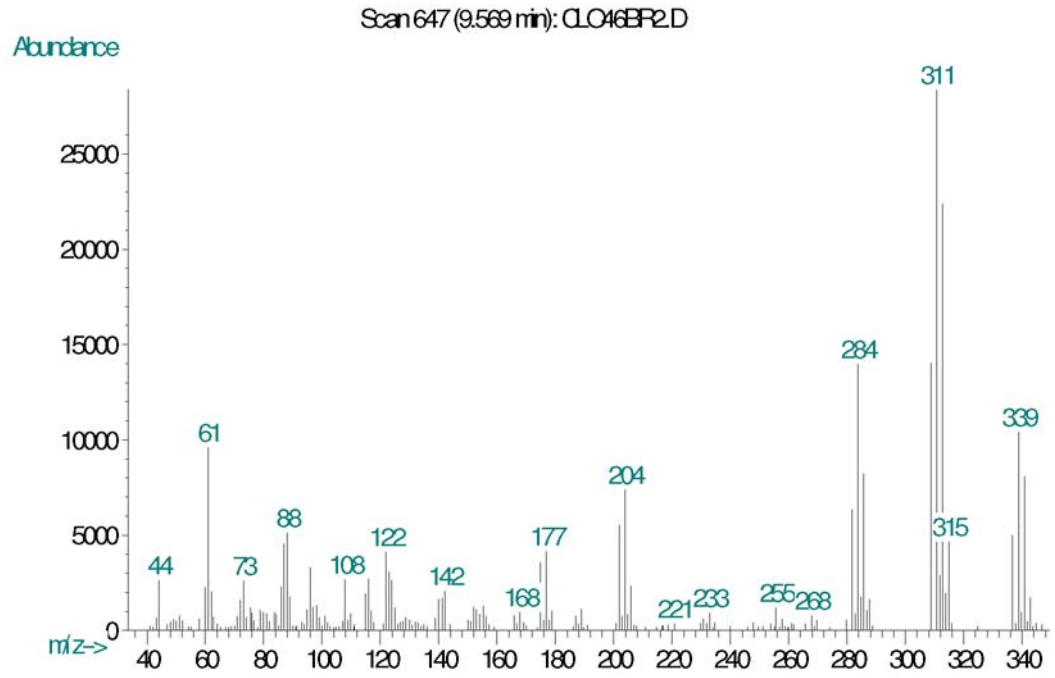

Figure S36. Mass spectrum of **11b**.

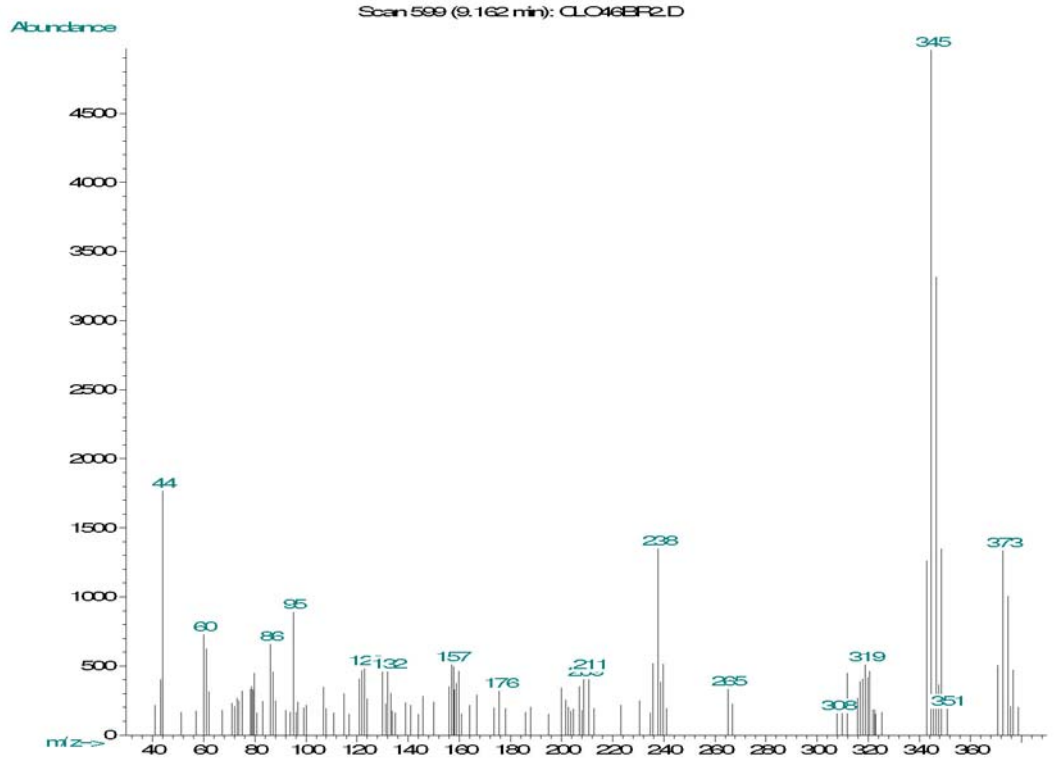

Figure S37. Mass spectrum of **11c**.